Radio detection of cosmic rays in the Netherlands
A feasibility study

F.J. Beens

Master's thesis for Physics & Astronomy

August 15, 2008

Supervisor: dr. C. Timmermans

HEN-465

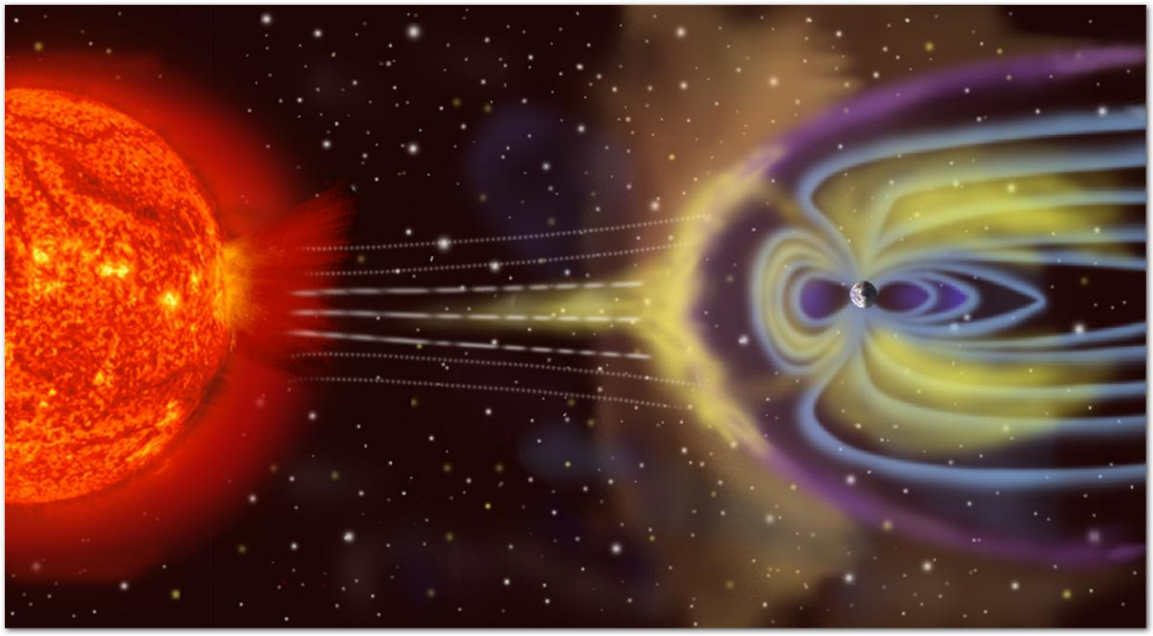

Radboud University Nijmegen

Institute for Mathematics, Astrophysics and Particle Physics

Preface

L.S.

This is my master's thesis. I worked on it at the department of Experimental High Energy Physics of the Institute for Mathematics, Astrophysics and Particle Physics at the Radboud University Nijmegen.
But before I begin, I wish to thank, first of all, my supervisor Charles Timmermans, for all his help and support. I also thank all of my friends and colleagues here in general and especially Marcel van Kessel, José Coppens, Harm Schoorlemmer, Raoul de Rooij and Irene Niessen, for creating a great atmosphere and being there during some difficult times for me. And last but not least, of course I thank my parents for everything! Thanks!

Freddy

Abstract

In this study we want to investigate the possibility to use radio detection of cosmic rays here in the Netherlands. In remote areas like Argentina this technique is being used already, but in Nijmegen we have to overcome a lot of background noise, like FM radio and TV transmissions, pagers and mobile phones.
In the first chapter we will look into the theory behind air showers and the detection of their radio emissions. In chapter two our experimental setup is described. This setup resembles the original setup in Argentina, the data of which is discussed in chapter three. The fourth chapter deals with the noise situation in Nijmegen, and first data of this setup is discussed in chapter five. Finally, conclusions are drawn in chapter six.
Hopefully the conclusion will be that it is a useable technique in more populated areas as well, but… we will see.

Contents

1 Theory

In this first chapter we will look into the theory behind extensive air showers and the ways to detect them, most importantly through radio emission. This chapter is largely based on "Radio Emission from extensive Air Showers" chapter III by H.R. Allan.

1.1 Introduction

In 1964 radio pulses from extensive air showers were observed for the first time. However, there are still quite a few open questions regarding their origin and possible applications. Thanks to ever improving radio techniques, the detection of cosmic ray radio pulses has now become possible under increasingly bad circumstances.
Classically particles in air showers are detected using detectors at the Earth's surface. These may consist of photo-multipliers and scintillator materials such as phosphor, or water generating light through the Čerenkov effect. But, even though these are rather effective means, it is even more direct to simply use the air itself through which the shower moves and the scintillation or Čerenkov light that is emitted here.
However, these faint light sources are only detectable under favorable conditions, i.e. cloudless moonless nights, whereas radio detection does not suffer from this drawback. The question now becomes if there is enough radiation produced at low frequencies, especially since for wavelengths beyond the distance between individual particles, the opposite contributions from positive and negative particles cancel each other. But thanks to the fact that most shower particles have relatively low energies, processes like Compton recoil result in a considerable negative charge excess. Instead of cancellation, coherence now results in a substantial increase in the radiation intensity at the lower frequencies.
So in 1964 Jelley *et al.* [1965, Nature 205, 327-328] tried to detect radio emission from air showers, assuming that the main mechanism was Čerenkov radiation. Using an antenna system consisting of 72 horizontal dipoles focused at 44 MHz, some radio pulses were found in coincidence with air showers, even though the energies received were only a fraction of the estimated energies.
While this does show that air showers can be detected by their electromagnetic radiation, it does not mean the dominant radio producing mechanism is Čerenkov. In fact charge separation in the Earth's magnetic field by the Lorentz force is a larger effect. This deflects the positively and negatively charged particles from each other, starting all over again at each pair creation. After many generations the result is an average separation, causing a transverse electric dipole moment moving through the atmosphere, producing radiation with energy proportional to $\nu^2\, d\nu$, instead of $\nu\, d\nu$ for Čerenkov radiation produced by a moving charge.
This average charge separation also causes a short element of current to move, perpendicular to its length, through the atmosphere, which in its turn is the cause of an electromagnetic shock wave, just as Čerenkov radiation, with the exception that its nature is magnetic instead of electric and polarized parallel to the current instead of radially. Finally the acceleration of the positive and negative particles under the influence of the Earth's magnetic field causes geo-synchrotron radiation. The relative importance of these four mechanisms was calculated to be first geo-synchrotron, then the transverse current,

the charge excess and finally the electric dipole, primarily at high frequencies and close to the shower axis.
These calculations were however still mainly based on Čerenkov-like radiation, neglecting longitudinal spread or disc thickness and end-effects. A more realistic approach considered the transfer of energy and momentum from the primary cosmic ray particle to the secondary particles and from these to the atmosphere through excitation and ionization by the Coulomb force and, especially at high altitude, deflection by the Lorentz force. Even though the atmospheric refractive index was neglected, the result was much closer to reality. By taking the disc thickness into account it was now found that the dominant frequency range in the electromagnetic pulse is between 2 and 50 MHz, depending on the altitude at which the shower develops.

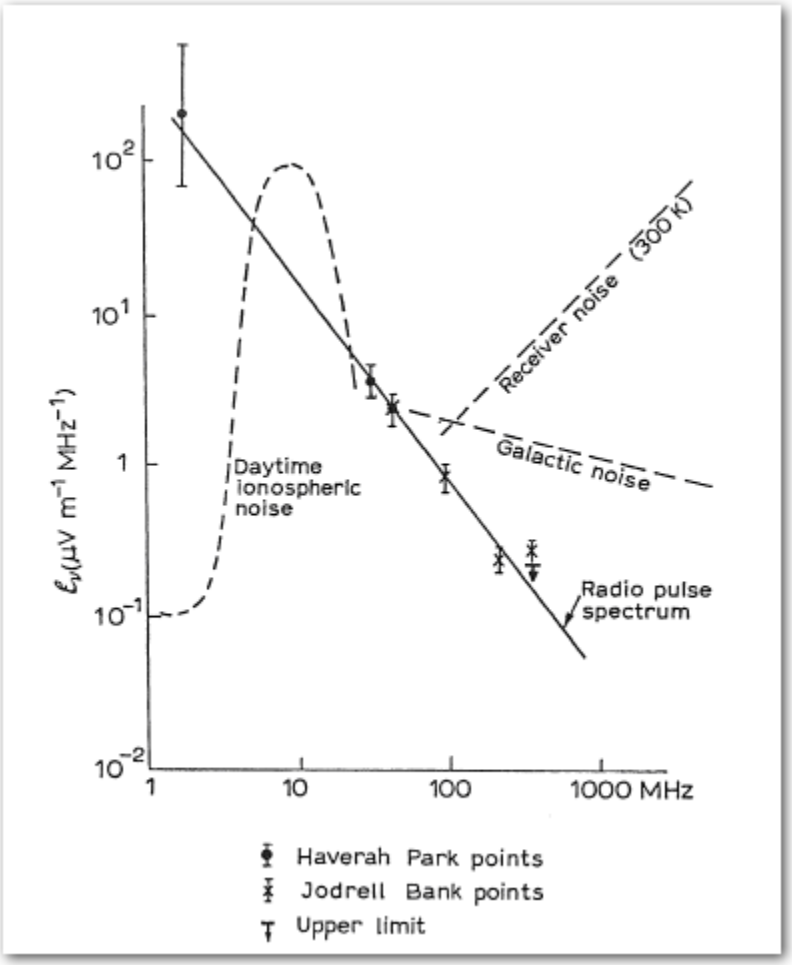

Fig. 1. A tentative radio pulse spectrum.
Detection threshold for bandwidth of 1 MHz and antenna gain = 1.

This agrees with the available experimental data (figure 1), showing radio pulses between 2 and 550 MHz, with pulse amplitudes falling off as the inverse of the frequency. Background noise further limits the most favourable range to between 30 and 50 MHz; just where the first experiment was sensitive.
In the end the goal is to use radio receivers as an alternative to regular particle detectors, because they can cover a large collecting area and do it cheaply. This is very important if

you want to capture large showers with energies around 10^{20} eV, which is interesting to many different astrophysical and cosmological models. It is also important because larger showers have fewer problems with background noise, so that it may become reliable enough to use only radio to detect these extensive air showers. Finally, a combination of both radio receivers and particle detectors is important too, especially when trying to identify the primary particles, because one expects heavy primaries to have larger but shorter radio pulses with more high frequencies, but fewer particles at ground level, since their showers develop more quickly and only the particles at high altitude contribute to the radio pulse.

1.2 Air showers: detection and structure

Thanks to the shielding of the Earth's atmosphere, only highly energetic particles reach sea-level. Muons for example, which are decay products of secondary pions, must have an energy of at least 2×10^9 eV when they are created. The primary particle energy must be even higher: typically 10^{10} eV. If you want to observe these directly you have to go high in the atmosphere, where more particles are able to get through. But even there you can not get much beyond 10^{14} eV, because of the small flux.

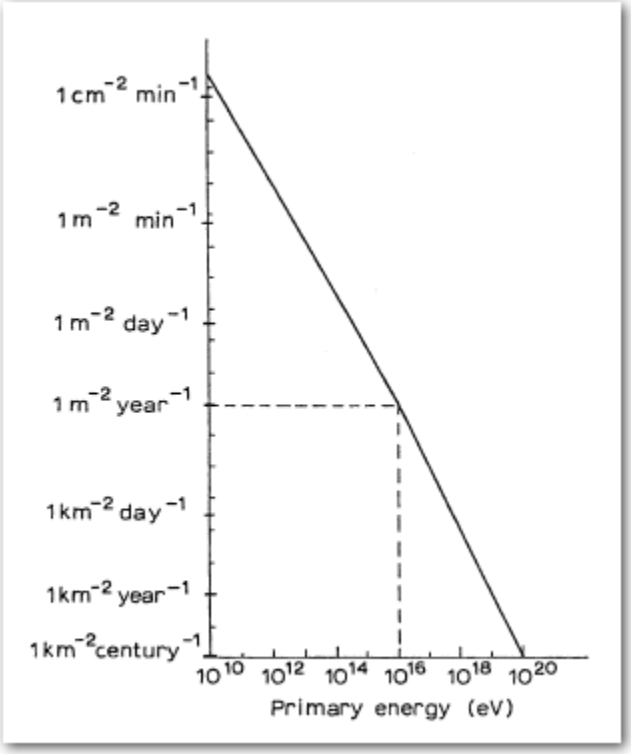

Fig. 2. Energy spectrum of the primary cosmic radiation

Thankfully there are other ways to detect these high energy primaries. Through a succession of nuclear and electromagnetic interactions a great number of secondary particles are formed, which can diverge up to more than 1000 m from the original shower axis. Now you can use an array of widely separated smaller detectors to cover a much larger area and reconstruct the event from these observations.

You can, for example, determine the original direction from the relative arrival times at the different detectors, keeping in mind that the shower front is slightly curved and has a finite thickness. The position of the axis follows simply when you assume circular symmetry of the particle density distribution. The primary energy can also be determined, but then you need to know how the number of charged particles varies with depth. And finally the primary mass is the most difficult. Different methods have been proposed for this, but the most promising is to measure the shower depth where the maximum number of secondary particles is, i.e. the shower maximum.

To determine the primary energy in a calorimetric way, you need to calculate the total track length of all the charged secondaries, which are responsible for loosing the greater part of all this energy. A secondary looses roughly 2×10^9 eV in one thickness of atmosphere. Thus it is important to know how the number of secondaries varies with the depth in the atmosphere. To learn this, the number of particles in showers that occur at the same rate per unit area is measured at different depths in the atmosphere. In this way the depth where similar showers reach maximum development can be determined. As the shower size and the primary energy increase, this maximum occurs at greater depths and for showers with around 10^{10} particles it reaches sea-level. For all shower sizes however, the so called effective shower length is roughly equal to one atmospheric thickness. By multiplying this with the maximum number of particles you get an approximation of the total track length to an accuracy of around 30%. Taking into account the ionization loss of the secondaries, the final result for the primary energy then is:

$$E_\mathrm{p} = 2 \times 10^9 \, N_\mathrm{max} \ \mathrm{eV}. \qquad (1)$$

So as long as you have an array at the appropriate depth to measure N_max, you can use this formula to calculate the primary energy. For measurements lower in the atmosphere additional approximations have to be made, resulting in a formula based on the average behavior of showers with a primary energy of around 10^{16} eV, measured at sea-level:

$$E_\mathrm{p} = 10^{16} \left(\frac{N}{10^6} \right)^{0.85} \mathrm{eV}. \qquad (2)$$

However most showers do not really follow the average behavior: as the primary interaction and therefore the start of the shower can take place at quite different depths, N may vary by a factor of 30, depending on the weight of the primary and the depth of the measurement. The muon distribution on the other hand has its maximum slightly below sea-level, so their number fluctuates less. By shielding the detectors from the electrons you can thus determine the primary energy at the surface more reliably.

To understand the radio emission, the shower structure needs to be known in much more detail. First, the primary particle does not transfer all of its energy in one interaction uniformly to the secondaries, but about half of it continues in a leading particle every single time, i.e. the inelasticity is only about 50%. This means that after ten interactions and almost one atmospheric thickness the leading particle still has roughly 1/1000th of the primary energy. The secondaries loose energy as well, because of further cascading and ionization. Depending on the primary energy their number reaches equilibrium around sea-level, meaning the secondary cascades must have a short length compared to the atmospheric thickness. In a very simple model these secondaries are primarily pions, π^+, π^- and π^0 in equal numbers, between 3 and 1000 in total per interaction depending on

the available energy. The energy is roughly equally shared between all of them. After about three interactions, their energy is so low that the probability for decay exceeds the probability for further interactions, and the production and decay come into equilibrium. The π^+ and π^-, mostly with low energy, decay into muons, μ^+ and μ^-, which now traverse the remaining atmosphere to sea-level almost without change and carry useful information about particle numbers and primary energy. Their number, or even better the proportion of high energy ones, also carries information about the primary mass, as heavy nuclei split into a number of lower energetic cascades decaying at an earlier stage.
The π^0 decays almost at once into two photons, which give rise to the electrons and positrons in the shower. These outnumber the other particles by an order of magnitude and are largely responsible for the radio emission. The electrons lose their energy by bremsstrahlung and the resulting photons create more electrons and positrons by pair production. In a rough approximation this means that the number of particles is doubled every 30 g cm^{-2} and the energy per particle is halved, until it reaches the critical energy: around 100 MeV in air. This energy and therefore maximum development of the cascade is reached after around 300 to 400 g cm^{-2}, after which the photons give their energy to electrons by Compton recoil and the particles lose theirs by ionization. This results in an effective length for the electron-photon cascades of around 500 g cm^{-2} and, depending on the original gamma energy E_γ^0, a maximum number of particles of:

$$N_{\max} = \frac{E_\gamma^0}{10^9}. \tag{3}$$

Around ¾ of the total track length belongs to particles with energies below the critical energy and the median energy is about 30 MeV. Taking this into account, adding the fact that there is overlapping of the generations and many different electron-photon cascades, the number of these so called soft component particles near shower maximum is:

$$N(>E) = N_{\max}\frac{30}{E+30} \qquad (E \text{ in MeV}), \tag{4}$$

for particles with an energy greater than E.
However, thanks to the fact that, through interactions between the cascade and the atmosphere, additional electrons of high energy are ejected from the outer shells of atoms and some of the positrons decay in flight, there is a considerable negative charge excess. When these ejected electrons have sufficient energy to produce ionization trails of their own, they are called δ-rays. About 1 MeV per g cm^{-2} is lost this way, of which 20%-40% through δ-rays of energy > 1 MeV. No less than 10% of the effective charge excess is thus caused by these δ-rays. About the same percentage is caused by photons, producing negative Compton recoil electrons instead of positive-negative pairs when their energy falls. And finally around 5% is caused by positron annihilation. In reality the Compton recoil part is more dominant, and all of this primarily at relatively low energies, so it will not be of great significance for the observed radio emission.

The lateral spread of the different shower particles is of great importance for the development of the radio signal, creating a shower disc of around 100 m wide and 2-3 m thick at sea-level. This lateral spreading is primarily caused by multiple scattering of electrons and a non-zero angle of emission of secondary particles in the case of nuclear-active ones and muons.

The nuclear-active particles remain within a few meters of the axis, with a transverse momentum that can be estimated using the uncertainty principle, giving $p_T \approx 400$ MeV/c. Only at very high energies this may be more. The longitudinal momentum ranges from around 10^{10} eV/c for the charged pions to between 10^{12} and 10^{13} eV/c for the zero-charged pions, which produce gammas. The corresponding lateral displacement of the π^+ and π^- before decaying into muons is only about one meter. Other nuclear-active particles can get as far as 10 m from the axis, but they have too little energy to be an important source of secondaries.

The muons, being produced at 6-7 km high, can travel 240-300 m from the axis before reaching sea-level. Because of this they already lag around 5 m behind the leading particle. But on average they also lag another 10 m because they are losing energy, slowing them down compared to the leading particle. When combining all effects, the disc thickness turns out to be a few meters near the shower axis, where the muon energy is high, and more when going away from the axis. Note that the muons play only a minor role in the radio emission.

The electrons are extremely important for the creation of radio emission. At each scattering a transverse momentum is imparted to them, which can again be estimated using the uncertainty principle. The scattering angle is about 0.17 radian when the electron energy reaches 100 MeV and 0.45 radian at 20 MeV. The overall r.m.s. lateral displacement at sea-level is about 50 m at 100 MeV and more at lower electron energies. The lag is about 3 m for electrons of 100 MeV, which is mainly due to scattering. At these energies, close to the shower axis, the electron disc is thus in front of the muon disc, whereas at distances of some hundreds of meters from the axis, where the electron energy is low, it is the other way around, because of the small curvature of the muon disc.

The external magnetic and electric fields cause a curvature when the shower axis is perpendicular to those fields. For particles with energy E MeV the magnetic field causes a radius of curvature $\rho = 100\,E$ m, whereas the curvature caused by the electric field is only around 1% of that, except during thunderstorms. For muons this results in an appreciable lateral deflection $D_m \approx 100 / E$ m (E in GeV) at sea-level, in opposite directions for positive and negative muons, causing considerable charge separation. The longitudinal lag can safely be ignored. The effect on the electrons (with a terminal energy E_T) is a lateral deflection $D_m \approx 1300 / E_T P^2$ m (E in MeV) at sea-level, which exceeds the scattering deflection only at low pressures $P < 0.3$ atmospheres. The longitudinal lag due to magnetic deflection is also only of importance at very low pressures, early in the shower development. At sea-level the electron and muon lag can thus be assumed to be controlled by scattering rather than magnetic deflection.

1.3 Radio emission

How is radio emission related to all these moving charged particles and what aspects of the shower structure, like the longitudinal development, can be inferred from the radio measurements? Because quantitative precision is less important here, the Feynman formulation of electrodynamics is used. For each charged particle in the shower, the wave amplitude is approximately given by:

$$\mathcal{E} = \frac{e}{4\pi\varepsilon_0 c^2}\,\ddot{\theta} = 1.5 \times 10^{-26}\,\ddot{\theta} \quad \text{V/m.} \tag{5}$$

The length of a pulse is related to the maximum frequency at which the radiation from different parts of the shower is still in full coherence as $\tau \approx 1/(2\pi\nu)$.
To an observer right on the shower axis the pulse length is zero, but when the distance from the axis is 10 km, the length is approximately 30 μsec. For air shower arrays, the relevant distance is more like a few hundred meters and the pulse length is considerably less. In an extremely simplified shower model where the shower begins at a height of 10 km, reaches maximum development at 5 km and has decayed appreciably at about 1 km altitude, the time interval between the beginning and maximum development is some ten times shorter than from the maximum until the end. This means that the pulse length associated with the build-up is much shorter and therefore the contribution of higher frequencies is larger than for later stages of development. In other words high frequencies tell about the shower growth, whereas low frequencies also tell about the decay.
But radial displacement, longitudinal lag and refractive index must be considered as well. Longitudinal lag has the biggest impact on path length differences close to the shower axis. Radial displacements are more important as the distance from the axis increases, but the geometrical effect dominates as soon as the distance reaches a few hundred meters. The effect on the actual pulse length depends almost entirely on geometrical path length differences even close to the shower axis, as longitudinal lag is not associated with apparent angular acceleration of charge, which is necessary to produce radiation. The refractive index reduces path length differences marginally, by about 1 m, which is not enough to upset the correct temporal order.
To estimate the magnitude of the radiation field, all kinds of charge motion need to be considered. Multiple scattering causes a time lag of approximately the longitudinal lag Δ_l divided by c and a lateral displacement r, changing the apparent angular bearing of each particle by about $r/L_{\max}$, where $L_{\max}$ is the height of the shower maximum. But the contributions to the field from these separate particles should be added together as in a random walk, through the sum of squares, making the net effect from n particles only $n^{1/2}$ as great as that from one. The effect of the Earth's magnetic field on an electron of energy E MeV, when the shower axis is perpendicular to it, is an angular displacement θ of about $1/E$. In this case however, the individual electric fields all point in the same direction and can therefore simply be added. The geomagnetic deflection has no appreciable effect on the time lag. In the simple model, where the number of shower particles is doubled and their energy halved every generation, this results in an angular polarization $P = ne\theta = eE_p/E^2$, with the energy E and the primary energy E_p expressed in MeV. But not all particles are actually charged and ionization loss discharges even more, so when that is taken into account, coupled with the formula for the time $t = l/c$ in which the angular displacement takes place, this leads to:

$$P = 10^{-3}\, eE_p t, \tag{6}$$

with E_p in eV, P in electron-radians and t in seconds. The radiation field can now be calculated from formula (5) in which the second derivative of $P = ne\theta$ replaces the second derivative of $e\theta$ to take care of a changing amount of charge:

$$\mathcal{E} = \frac{1}{4\pi\varepsilon_0 c^2}\,\ddot{P} = 1.5 \times 10^{-26}\,\frac{d^2}{dt^2}(n\theta) \quad \text{V/m}. \tag{7}$$

When this crude approximation is plotted, it is clear that the result is zero except at $t = 0$, meaning that even though the disc thickness l is finite, the actual radio pulse is a true δ-

function in time here. To calculate the magnitude of this pulse, which is the same for all frequency components within the pulse, a Fourier transform can be used and this finally leads to:

$$\mathcal{E}_\nu = 2 \int \mathcal{E}(t)\, \mathrm{d}t = 3 \times 10^{-26} \frac{d}{dt}(n\theta) = 3 \times 10^{-23} E_\mathrm{p} \quad \mathrm{V\ m^{-1}\ MHz^{-1}}. \tag{8}$$

This formula provides an estimate of the field strength of the radio signal due to a shower of primary energy E_p expressed in eV. For primary energies > 10^{17} eV, the predicted field strength on the shower axis is then > 3 μV m^{-1} MHz^{-1}, which is quite compatible with the experimental data.

But in reality the pulse is not a true δ-function, because the refractive index correction of ~1 m in path length causes the radio pulse to be spread over ~1/c seconds. Once the period starts to become comparable with this length, at about 50 MHz, the frequency components begin to fall off. This effect is appreciably reduced at distances between 100 m and 200 m from the axis, but still a spread remains, causing $\mathcal{E}_\nu$ to fall off at ~100 MHz. At distances R > 200 m geometrical path length differences take over and the fall off frequency is $\nu_{max} \sim 10^6/R^2$ MHz. This value however depends on the altitude of the shower maximum, increasing when the maximum gets higher. Measuring ν_{max} could thus be a way to establish the height of the maximum and thus the primary mass. Finally, the time lag causes a so called overswing after the δ-function, exactly balancing the area under the δ-function, making sure the total radio pulse contains no d.c. component.

1.4 Detection of radio pulses

As can be seen from formulas (5) and (7), the electric field $\mathcal{E}$ is related to the movement of charged particles. The duration of the pulse can be estimated by considering the transit time of the shower through the atmosphere, combined with a kind of Doppler shortening when the shower moves towards the observer; the latter holding primarily for the earlier parts of the shower development. This causes the decay to last at least 10 times longer than the build-up to shower maximum and both increase with the distance from the axis proportional to R^2. The amplitude for very low and very high frequencies is small, or in fact zero for the zero-frequency component. For intermediate frequencies, $\mathcal{E}(t)$ can be considered as a single pulse of length τ, the time taken for the build-up to maximum. The amplitude in the range from 1 to 10 MHz is independent of frequency and given by the integral in formula (8), with t ranging from 0 to τ. For higher frequencies it falls off as the inverse of the frequency. This amplitude is proportional to the sine of the angle between the shower axis and the magnetic lines of force and, if full coherence is maintained, also to the primary energy.

An ideal radio receiver should be sensitive to all these frequencies, ranging from near d.c. to ~100 MHz. However, it would also be sensitive to a lot of background interference. Therefore the bandwidth has to be limited, resulting in a distortion of the observed pulse shape.

In a simple receiver, consisting of a metal plate of area A m^2, connected to a junction transistor acting as a charge sensitive amplifier, the collector current is determined by the amount of charge fed into the base and ideally would follow the changes in the radio field strength $\mathcal{E}$ faithfully. However, when the effects of inductance are included, or a tuning coil is introduced, the received signal is distorted. A short pulse now causes an

oscillation, with an amplitude proportional to $\mathscr{E}\tau$. The measured amplitude is determined by the current $i_0 = \mathscr{E}\tau\, s/L$, caused in the inductance in time τ by the pulse. By using the resonant frequency f_0 of the aerial system, the amplitude can be expressed as:

$$q_0 = 2\pi\,\varepsilon_0 A f_0\,(\mathscr{E}\tau). \tag{9}$$

The resulting collector current is given by:

$$i_c = 4\pi^2\,\varepsilon_0 A f_0 f_T\,(\mathscr{E}\tau), \tag{10}$$

with f_T the gain-bandwidth product for the transistor. The number of oscillations can be limited by introducing a resistance, not greater than necessary for critical damping, in series with the inductance L. This way any receiver based on a single resonant circuit with natural frequency $f_0 \ll 1/\tau$ would be enough, if one is only interested in the total pulse. If the receiver has a linear detecting stage, the output displays the envelope of the damped sine wave, which is a single pulse of duration $\sim 1/\pi\,\delta f_0$, with δf_0 the bandwidth of the resonant peak. However, even though the resistance can be tuned to critical damping ($R \sim 2\omega_0 L$) to limit the oscillations and prevent resonant amplification of periodic signals near f_0, it has no influence on low frequencies, where most interference problems occur.
To improve this effectively, a band-pass filter is called for. When such a filter is being used, removing all frequency components except those in a range δf about a central frequency f, the remaining components will add to give a maximum output at $t = 0$ proportional to δf, but oscillate at frequency f away from $t = 0$:

$$V \sim \sin(\pi\,\delta f\, t) \,/\, (\delta f\, t). \tag{11}$$

So the smaller the bandwidth, the more the signal is distorted by these oscillations. The signal is also delayed and this delay gets longer too when the bandwidth gets smaller, as well as when the filter is required to cut off the pass band more sharply. On top of that the delay is frequency dependent.
To conclude, the better the discrimination against interference has to be, the more the pulse shape is distorted. The output voltage is proportional to the bandwidth δf, as well as to the impulse of the radio pulse in formula (8) provided τ is small compared to $1/f_0$, and the duration is of the order of $1/\delta f$. Also the energy contained in the output pulse is proportional to the bandwidth, as $V^2 \propto \delta f^2$. The output voltage due to noise however, varies only as $(\text{bandwidth})^{1/2}$ and therefore the same goes for the signal to noise ratio. A larger bandwidth would thus be best, if it were not for the fact that the noise is very large except over rather limited ranges of frequency. It is only in those ranges that there is a reasonable chance of observing the radio pulses at all.

The actual strength of the background depends on the frequency range under study. At low frequencies the noise from the ionosphere dominates, whereas at higher frequencies city or galactic noise and of course FM radio “noise” is most important. For frequencies greater than 100 MHz the intrinsic receiver noise is the limiting factor. For this receiver noise, the noise voltage v_n in a bandwidth $d\nu$ is given by:

$$v_n^2 = 4R\,kT\,d\nu, \tag{12}$$

which is independent of ν. The field strength $\mathscr{E}_\nu$ needed to overcome this v_n at the receiver terminals however, increases proportional to ν.
From 100 MHz down to 20 MHz the galactic noise takes over and its noise temperature increases from about 500 K to 50,000 K. The noise field strength however increases only by a factor 2. Below 20 MHz the noise rises sharply again, because here the ionosphere

reflects and transmits noise from thousands of miles away. But around the Larmor frequency (~1.5 MHz) spiraling free electrons are causing a daytime noise minimum.
Within 10 km from cities and settlements man-made noise coming from transportation and industry can greatly exceed the natural sources of noise from 20-100 MHz. And of course radio transmitters for telecommunication and other purposes are a substantial source of noise, but there are quiet gaps that widen for example at night. For these reasons most radio pulse experiments are carried out between 30 and 100 MHz, with bandwidths ranging from 2 to 20 MHz. Higher frequencies are being explored as well, at the cost of less coherence, just to be free from most man-made sources.

For a general antenna system the effective collecting area A is given by:

$$A = G\,\pi\,\lambda\!\!\!^{-2}\,, \tag{13}$$

with G the maximum gain, having a value of 1.6 for a half wave dipole. Larger values can be obtained by more elaborate arrays, to increase the effective collecting area approximately up to the physical area. Once G is known for a specific antenna design one can relate the field strength of the incident radiation to the voltage delivered by the antenna to the receiver input terminals:

$$V = \frac{c}{2\pi\sqrt{120}}\,G^{½}\,R^{½}\,(\delta\nu/\nu)\,\mathcal{E}_\nu \quad \text{V}. \tag{14}$$

But because the mean value of G, averaged over all directions, is 1 by definition, increasing the maximum means it decreases in other directions. As long as the direction of the signal is known, this improves the signal to noise ratio. When it is not accurately known, as may well be the case for many air showers, this causes uncertainty in the value of G and thus in that of the field strength. The minimum values, in the horizontal directions in case of high-gain antennas directed towards the zenith, are important for the background noise level given to the receiver.
Depending on the required gain and direction on the one hand and the size and cost on the other, the appropriate antenna design is chosen. For pulses coming from near the zenith an array of horizontal dipoles with suitable phasing, at best oriented along the geomagnetic E-W, above a conducting ground plane is convenient. For directions close to the horizon vertical wire antennas ¼λ long, more like those used in normal telecommunications, are the simplest choice, using corner reflectors to point them at a particular azimuth, although shorter ones may be necessary at low frequencies because of the cost. An alternative choice may be rhombic antennas. At frequencies above 100 MHz smaller sized highly directional antenna systems can be used, while being free from ground reflections.

Next come the amplification and rectification stages. But the rectified or “video” output of most short radio input pulses is limited by the receiver bandwidth, because its duration is given by 1/δf second. And it may also be somewhat delayed and accompanied by a number of satellite pulses, although this is not really a problem in practice.
The simplest way now to measure $\mathcal{E}_\nu$ is by using a linear detector, where $\mathcal{E}_\nu$ is proportional to the output pulse peak amplitude. But when the signal amplitude is comparable with the noise, the combination of both varies according to the phase and is no longer proportional to $\mathcal{E}_\nu$. As an alternative the d.c. component of the detector output can be monitored as a measure of the strength of the received signal. At frequencies with

only galactic background noise, this well known mean noise level can now be used to check the receiver performance.
But even though the mean noise level is hardly effected by them, short but frequent noise pulses of large amplitude may make the observation of the air shower pulses almost impossible. When triggered by particle arrays this is not really a problem, but when only radio methods are being used it is. In that case widely separated, independent radio receiving channels, with high enough threshold levels to keep the rate of random simultaneous pulses at a minimum, have to be used.

2 Setup

In this chapter the setup is described that we use for our measurements in Nijmegen in coincidence with the HiSPARC setup [hisparc.hef.kun.nl].

2.1 The trigger

General principle

The heart of the trigger consists of two particle detectors. These detectors are made up of scintillator plates with an area of 0.42 m^2 each, and read out by photomultiplier tubes. Each of these plates trigger on single muons at quite a high rate (about 100 Hz), but when requiring a particle in both of these plates the rate drops to about 0.2 Hz. The resulting triggers correspond to small local showers. As we wish to examine radio signals from larger showers, we are interested in correlated events over larger distances. Therefore, we use this setup in coincidence with the HiSPARC setup, and perform an offline check for coincidences. This can only be done if we have a precise timing measurement. The Trimble GPS-system provides this measurement. When using coincident events, the energy threshold is around 10 to 100 PeV.

The setup

A schematic overview of the setup is given here:

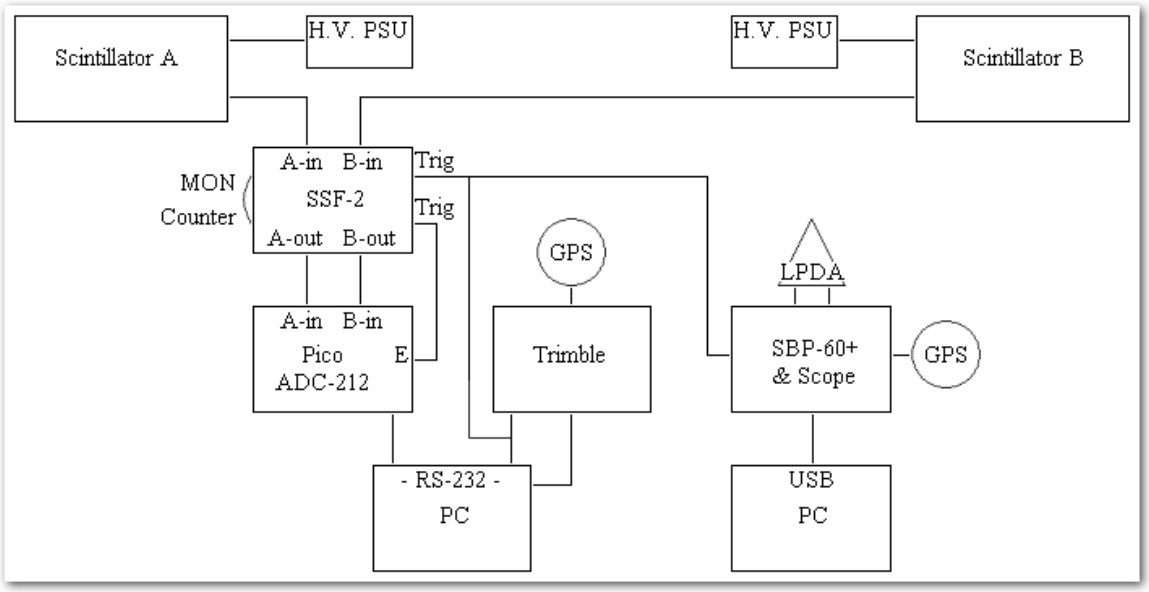

Fig. 3. The setup

When both scintillator detectors, which are located 4 m apart, detect a particle within 1.2 µs, the SSF-2 (Scintillator Signal Follower) sends a trigger signal (TTL) to an oscilloscope and GPS counter. The SSF-2 does not only create the trigger, but it also shapes the incoming signal by widening it. The width of the outgoing signal is better

matched to the 50 MHz sampling frequency of the Picoscope ADC-212. The trigger signal is also fed into the Trimble Acutime-2000 system, where it creates a timestamp. This timestamp, as well as the Picoscope data, is fed into a pc. On this computer, a LabVIEW program combines the data and timestamp. Furthermore, a Java applet sends the timestamped events to a remote server where the data is stored and combined with data from other stations.

2.2 The readout

At each external trigger, the antenna signal is recorded by the antenna readout. The antenna itself is a set of two wire LPDAs (Log Periodic Dipole Array), one for the North-South and one for the East-West polarization. An LPDA consists of a number of linear elements of different length, each resonant at a different frequency, thus creating an antenna sensitive to a wide band of frequencies.

Both its signals (from the North-South and East-West directions) are filtered using a commercial Band Pass Filter (SBP-60+). This filter limits the sensitivity to the frequency range between 55 and 67 MHz, to reduce the FM and low frequency noise. The frequency characteristics are shown in figure 4:

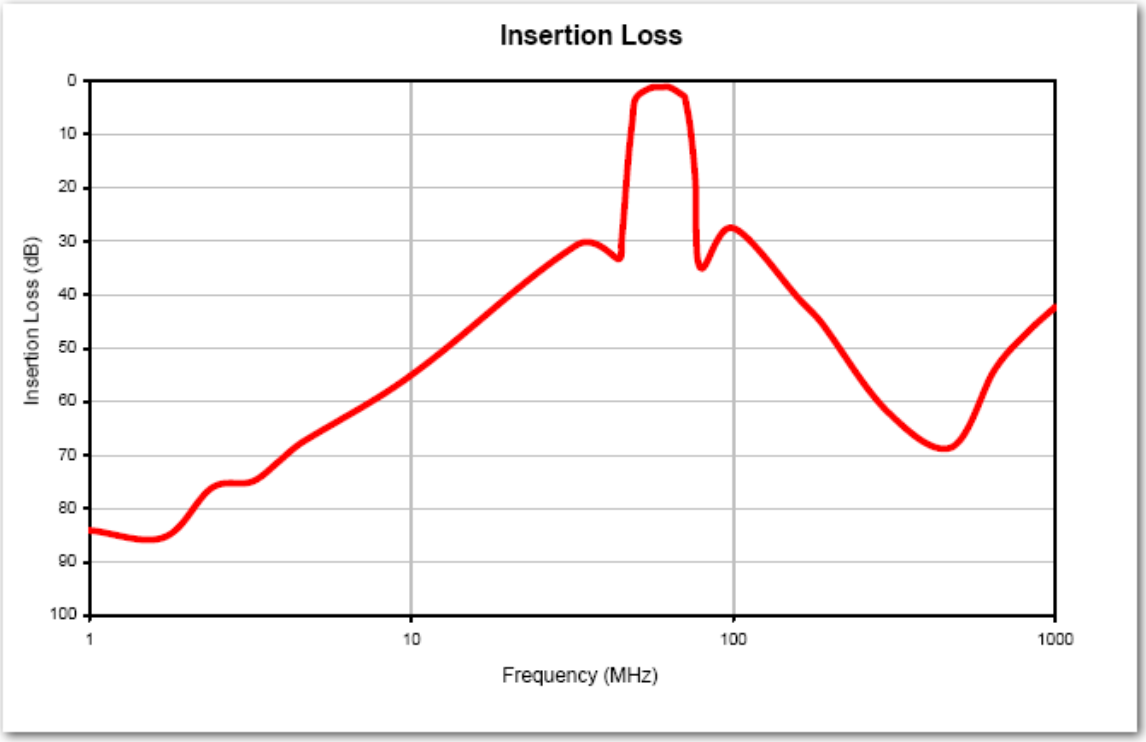

Fig. 4. SBP-60+ Characteristics

The filtered signal is amplified by 30 dB and fed into a custom made digital scope. This 12 bit scope has a sampling rate of 200 MHz and it has a GPS timing unit built in. A trigger produced by the SSF-2 is sent to the scope, which then stores a timestamp and two traces of 2000 points each, corresponding to 10 µs of data for both polarization directions. This data is transmitted to a mini-PC over USB, and stored onto a server using Ethernet. From there, the data is analyzed.

3 Data measured at the Pierre Auger Observatory

Before looking at the data taken by our setup in coincidence with the HiSPARC setup, we will look at data taken at the Pierre Auger Observatory in Malargüe, Argentina.

3.1 Introduction

This data set, which was taken in a period of about 9 months, consists of more than 300 events. These events were recorded using a setup similar to the one described before, however the antennas were connected to the readout using 160 meter long cables. In order to be able to drive the signal over these cables, a low noise amplifier with an amplification factor of 20 dB was used. The data set consists of only 300 events, because only those events recorded by the Pierre Auger Observatory were used. In this way, the energy, core position and direction of the primary particle are known. Even though the setup in Argentina is 1400 meter above sea level, one expects the data to be similar to results at sea level, at least within a factor of 2 [dr. Tim Huege, www.timhuege.de/reas].

3.2 Treatment of the data

The data recorded in Argentina are filtered between 50 and 70 MHz. The filtered pulse height will be fitted using an exponential, which is the following empirical formula (based on formula 84 in "Radio Emission from extensive Air Showers" chapter III by H.R. Allan):

$$\mathcal{E}_v = 200\, E_p \sin\alpha \cos\theta \exp\left(-\frac{R}{R_0(\nu,\theta)}\right) \quad \mu V\ m^{-1}\ MHz^{-1}, \tag{15}$$

with E_p the primary energy in EeV, α the angle between the shower axis and the Earth's magnetic field, θ the zenith angle and R the distance between the antenna and the shower axis. The parameter R_0 gives the scale of the lateral spread of the radiation, depending on θ and the frequency ν.

When fitting $\ln(\text{signal} / E_p) = -R / R_0 + A$, the parameter R_0 can be extracted. It was determined to be about 600 m. Earlier experiments have found values closer to 200 m, therefore this result was somewhat higher than we expected. This means we can detect showers from farther away than we originally thought. The A parameter gives the logarithm of the pulse height of a 1 EeV shower in the core position, assuming that the exponential function is an appropriate description.

As an example, the fit for the pulse height obtained using an LPDA in the North-South direction is shown in figure 5:

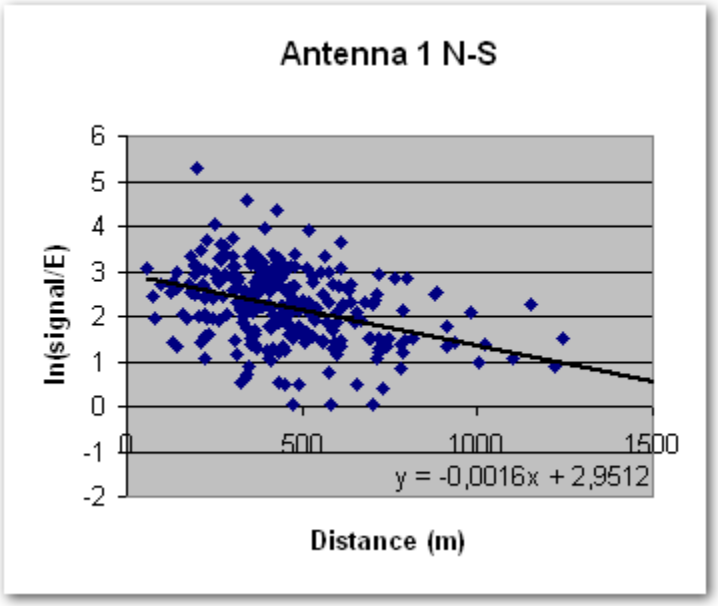

Fig. 5. Determining R_0

The average results for the N-S and E-W polarizations are shown in the following table:

Table 1

	R_0 (m):	A:
North-South:	625 ± 30	2.76 ± 0.20
East-West:	577 ± 30	2.93 ± 0.20

As we now have an approximate description of the dependence of the signal on R, we can create the quantity (signal / E_p) exp (R / R_0) and plot this vs. cos θ. A linear dependence would then be expected, and from the formula quoted above, with a slope of 200 sin α, or averaged about 141. But the result of the linear fit gives a slope of around 48, as can be seen in figure 6. One should also note the large spread of the data, which may originate from the dependence on sin α.

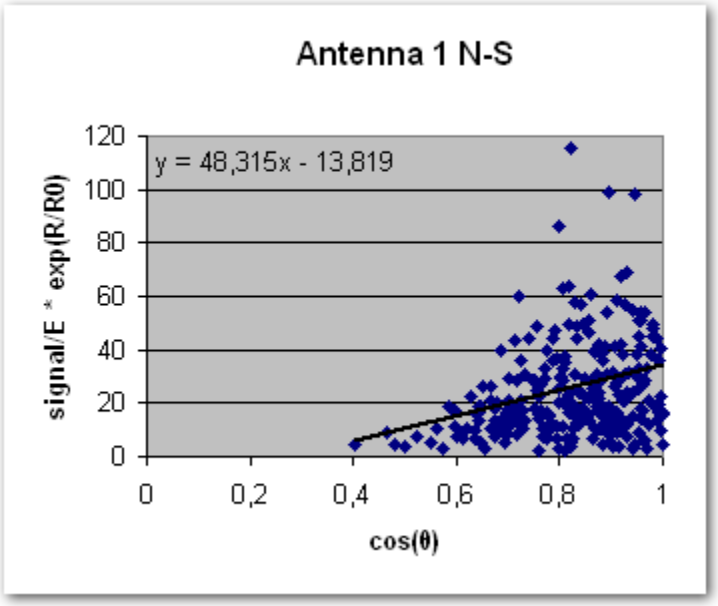

Fig. 6. Finding the θ dependence

Again, removing the observed θ dependence from the data by creating the variable signal / $(48\sqrt{2}\,E_p \cos\theta) \exp(R / R_0)$, we can determine the $\sin\alpha$ dependence, which should then give a slope of 1 of course. However, there appears to be no dependence on $\sin\alpha$ at all, as shown in figure 7:

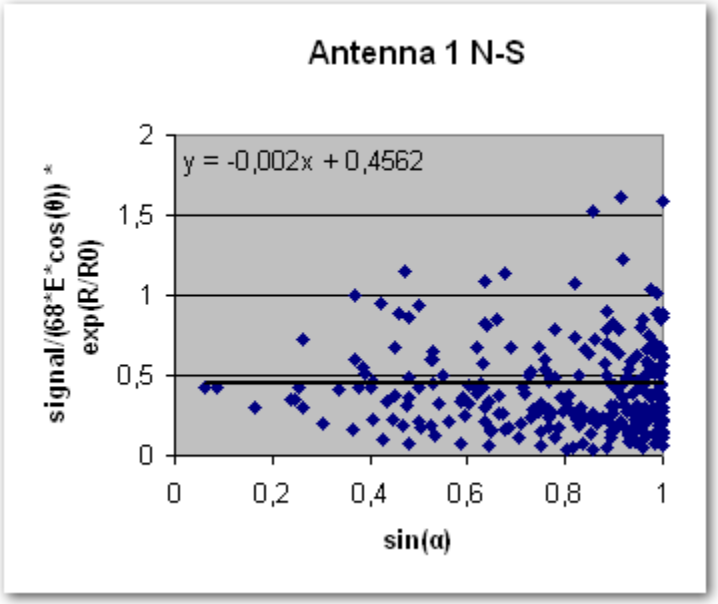

Fig. 7. Looking for the $\sin\alpha$ dependence

3.3 Relevance of this result

The observed dependence on R can be used to estimate the signal strength in Nijmegen as a function of energy and distance to the core. One should keep in mind that there are

large shower-to-shower fluctuations, but this does provide an indication of the distance out to which radio measurements can be made as a function of primary energy. This distance is calculated by assuming that the minimal detectable pulse height equals the noise value. Thus we get:

$$R = -R_0 \, (\ln (\text{noise} / E_p) - A). \qquad (16)$$

Examples for the Argentine setup are given in figure 8, using R_0 and A as listed in table 1. The background noise in Argentina is about 3 mV, so the plots show when a 3 mV signal is observed, as a function of shower energy and distance for primary energies between 0.1 and 12 EeV.

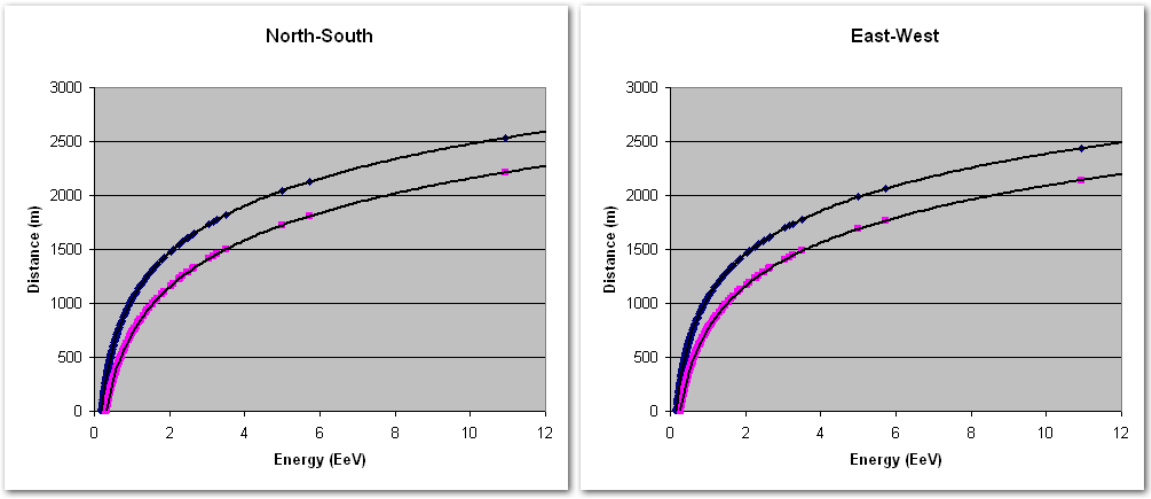

Fig. 8. 3 and 5 mV signals as a function of primary energy and distance to the core

As can be seen here when zooming in, showers with an energy below 0.16 EeV are not expected to be detected in Argentina.

We also show the results for a slightly higher noise level (5 mV). The direct impact on the range out to which showers can be detected is clear. In reality, the noise level fluctuates due to the visibility of the galactic center. Therefore, the sensitivity of single antennas is time dependent.

4 Noise measurement in Nijmegen

When measuring in a crowded area like Nijmegen, one needs to find out at what frequencies there is a low enough noise level to be able to detect any radio signals from air showers. And even more important: what frequencies have to be excluded, because the noise level there is just too high?
By using a spectrum analyzer connected to the LPDA antenna, we looked at the average and maximum noise levels in the North-South and East-West directions. The result can be seen here:

N-S Average N-S Maximum

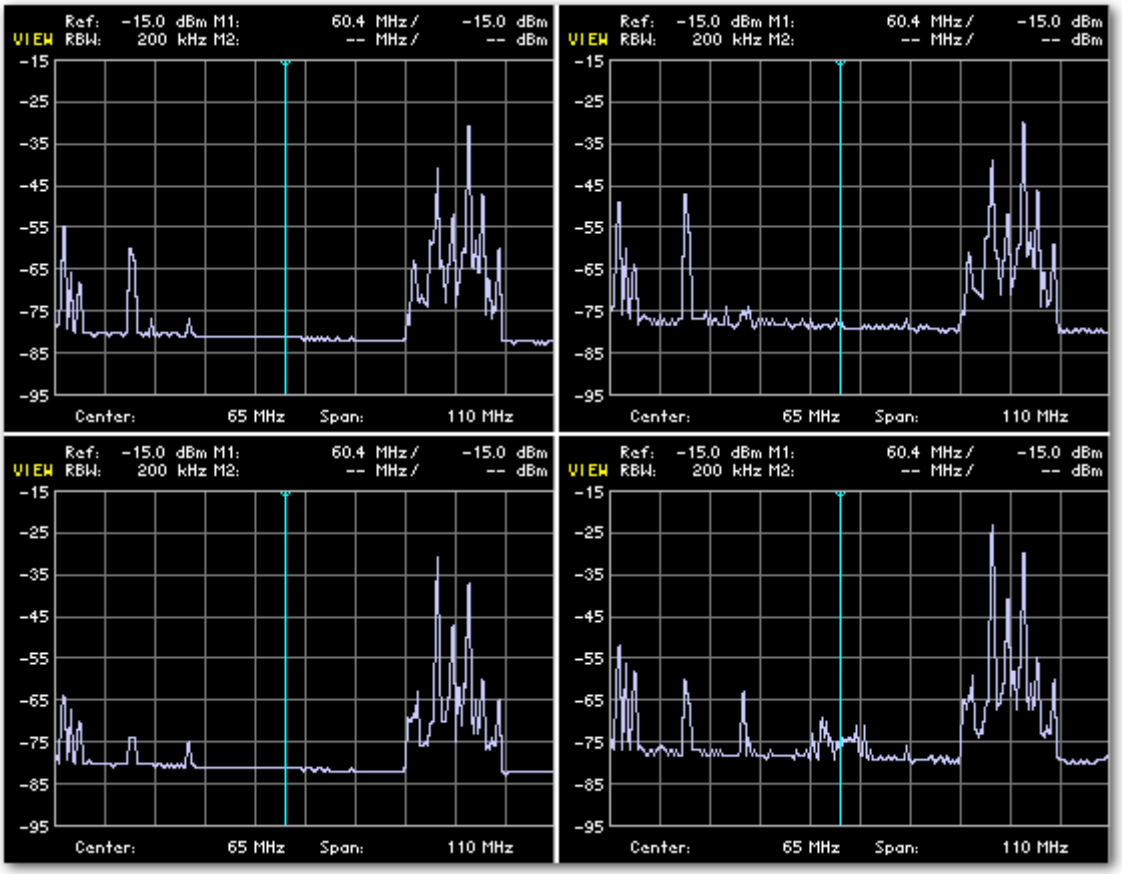

E-W Average E-W Maximum

Fig. 9. Noise level measurement

Some features are immediately clear. At low frequencies, below 17 MHz, one sees the short wave band radio. At about 27 MHz an additional peak can be observed and in some of the diagrams more smaller peaks are seen. In the range from about 41 to 87 MHz it is relatively quiet and from 87.5 to 108.0 MHz the FM band is clearly visible. This is all on top of the minimal noise level measured by the spectrum analyzer which, for this measurement, is set around -80 dBm/200 kHz. Note that this corresponds to a voltage level of 0.02 mV/200 kHz, or in our ADC a level of 0.2 ADC/200 kHz.

In order to be able to detect radio signals from showers, without being interfered too much by “noise” sources like FM stations, we need to limit our measurements to the quiet band which ranges between 41 and 87 MHz. The Band Pass Filter that we chose limits the sensitivity to the frequency range between 55 and 67 MHz, so that is well within safety limits. Chapter 2, figure 4 shows the characteristics of this filter. The suppression at the FM band is about 30 dB. As can be seen from figure 9, this does not yet reduce the noise level at the FM band to below the level in our region of interest. Therefore, we will apply a square digital filter between 50 and 70 MHz to our data before analyzing it. The disadvantage of this high noise level is the fact that saturation of the amplifiers plays a main role. This caused us to remove the 20 dB low noise amplifier at the antenna, and run with only 30 dB of amplification. Even so, after digitally filtering the data the noise level between 50 and 70 MHz is about 5 mV.

5 Radio detection of cosmic rays

5.1 Expectations

The results presented in figure 8 can be used to estimate the rate and minimal detectable energy in Nijmegen as well. In Nijmegen we do not use the low noise amplifier that is being used in Argentina, so we lack the 20 dB of amplification. On the other hand, as mentioned before, the background noise without the amplification is at just about the same level as in Argentina with amplification, or even slightly higher: between 3 and 5 mV. So it is obvious that the noise voltage level in Nijmegen is about 10 times higher than in Argentina.
We will thus simply use the same relationship between distance to the core and primary energy as obtained for the Argentine data. In order to estimate the range of the radio signal in Nijmegen, a noise level of 30 to 50 mV is used. The resulting plots are shown in figure 10:

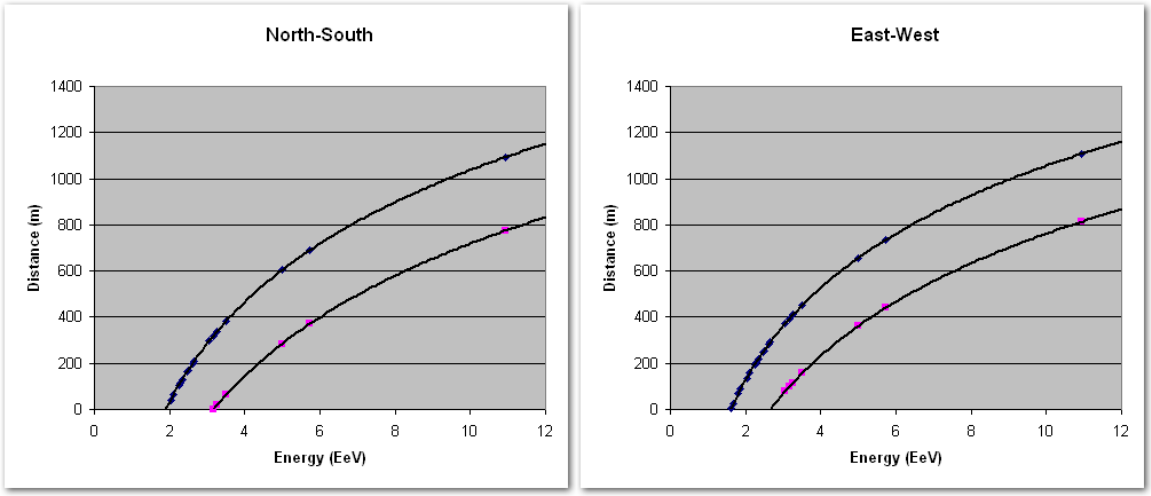

Fig. 10. 30 and 50 mV signals as a function of primary energy and distance to the core

These plots show that in Nijmegen we do not expect to detect any signals from showers with an energy below 1.6 EeV.

Next, we try to calculate the expected number of events per day. In order to make this estimate, we need to know the flux of primary particles in this energy regime. This flux has been well measured by the Pierre Auger Collaboration [ref. arXiv:0806.4302]. The flux follows a power law below 40 EeV, and has an additional suppression at higher energies. A plot of the functional description is given in figure 11:

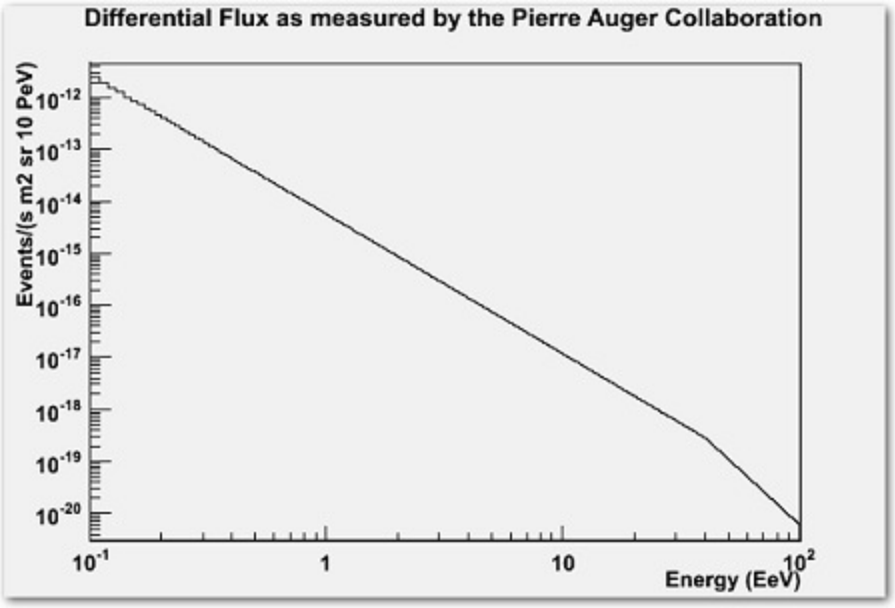

Fig. 11. The differential flux as a function of energy

Note that the lower end of this figure is below the minimal measured energy of the Pierre Auger Experiment. It extends to below the so-called ankle, and is thus too low. However, as we are interested in the higher energy domain, this is not a problem.

Now, the differential flux is multiplied by the sensitive area for the antenna. This sensitive area is taken as a circle with a radius depending on the energy of the shower, as given by the graph in figure 10. The result, assuming a 30 mV background noise level, is shown in figure 12. In this figure, an opening angle of 1 sr is used, and we have multiplied the rate from figure 11 by 86400 to get the number of events per day.

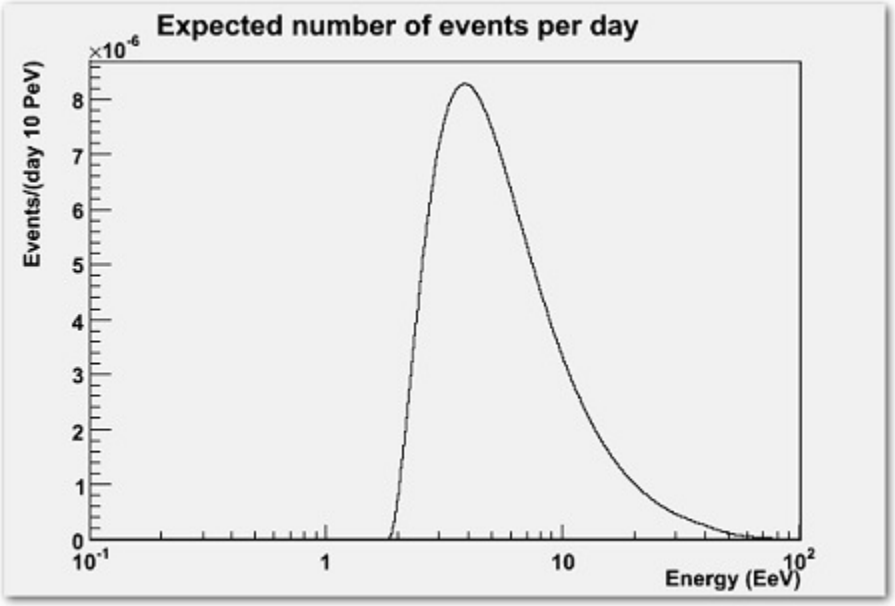

Fig. 12. Number of events per day as a function of energy

Finally, we simply integrate figure 12 to get the total number of events per day. The result is that we expect to detect only 0.0078 events per day at the noise level here in Nijmegen.

5.2 Event candidates

Then we could let the experiment run and we did so for 81 hours. During this time a great number of particle hits were registered by our setup, but only those that were concurrent with at least one HiSPARC station in the neighborhood were kept for further analysis, to make sure they really originated from a significant shower. And even this sample contains a lot of uninteresting events, not having the shower core nearby the radio antenna. You can tell by looking at the number of concurrent particles hitting the detector; when that number is too low, the shower was simply too far away for us to detect it reliably, especially considering the distance restrictions for the radio detection, as discussed above. As a measure we took 100 mV as the output of the scintillation detector, which corresponds to about 10 particles in 0.5 m^2. Anything below that was discarded as not significant.
For the selected events we looked at the signal recorded by our antenna and hoped to find some signals that would indicate a shower as well. But this too sounds easier than it is, as the trigger signal itself is recorded, which can be seen here:

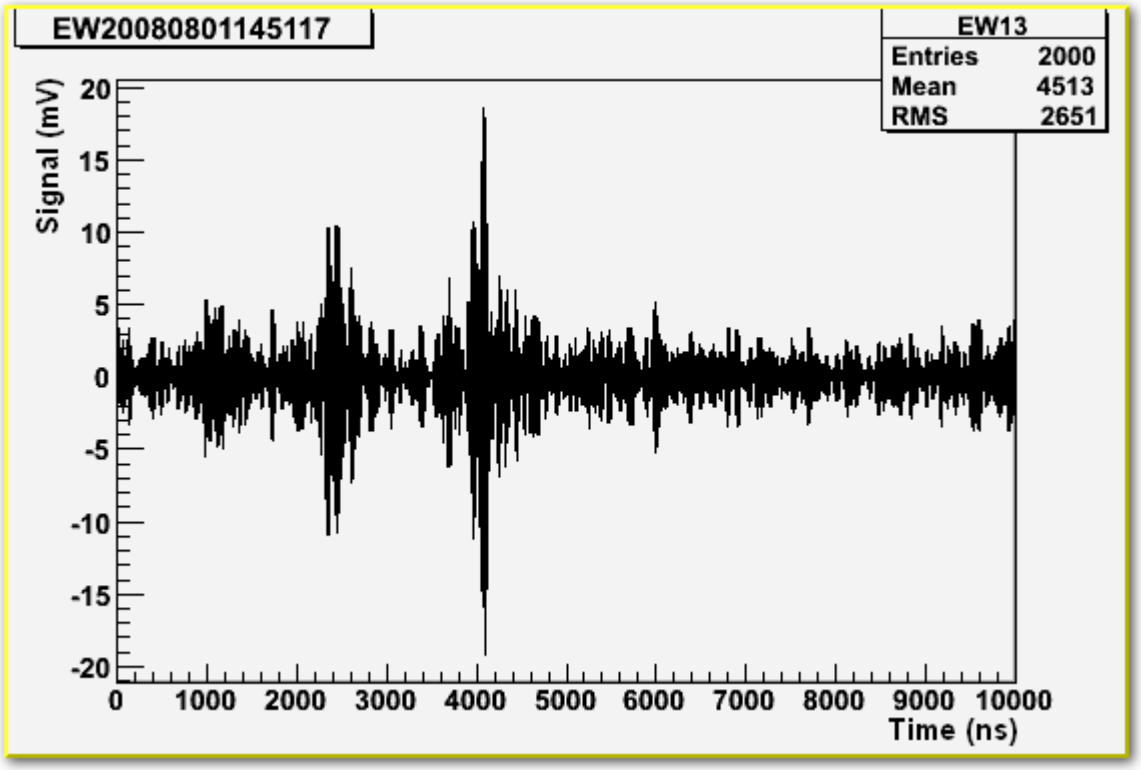

Fig. 13. The trigger visible in the radio signal

The two pulses around 2.4 and 4.0 μs are just the rising and falling edges of the trigger signal. Also clearly visible is the average noise level between 3 and 5 mV. So we are looking for pulses around 2.4 μs that are clearly higher than those from the trigger.

Pulses that answer to this description are very rare, as expected, but at least we found three, as shown in figure 14:

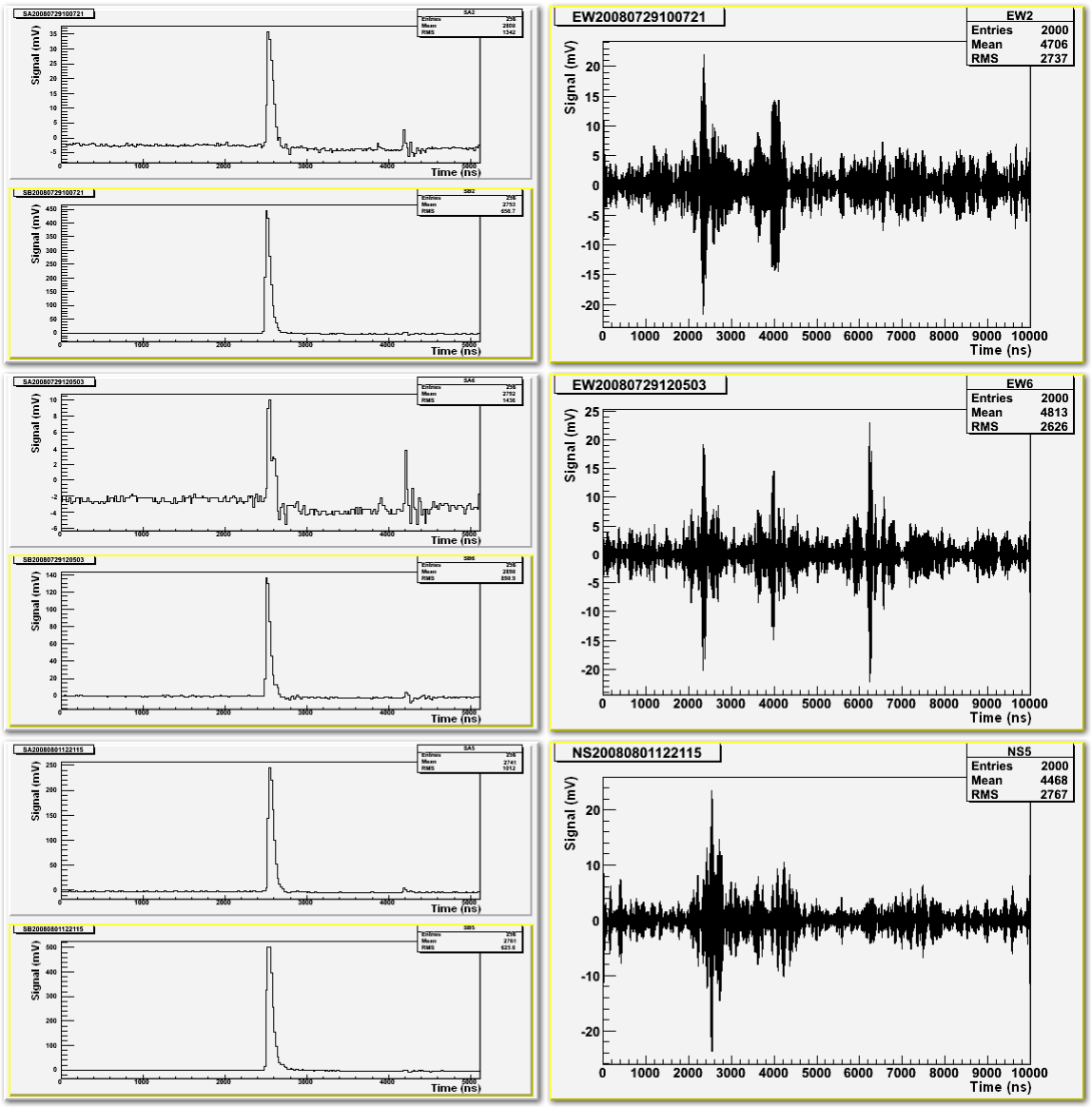

Fig. 14. Three suspected events. On the left the signals from the scintillator and on the right the radio data.

And even these three traces show only suspected signals, as one antenna is just not enough to know for sure if it really is from an air shower. So it is very likely, also considering our expectations, that at least one or two of these traces are not what we were looking for either.

All the other traces, with a proper trigger, but without a decent signal, of which we found 73 in total, are from showers with a primary energy that is just too low for us to detect here in noisy Nijmegen. The unexpected pulse around 6.2 μs in the second trace was even stronger in the N-S direction than it already was for E-W, so it is probably just a radio pulse from a terrestrial source.

6 Conclusions

Our goal was to see whether or not it is possible to detect air showers through radio detection in the Netherlands, where it is quite noisy in general. And while this is already hard in a quiet area like Argentina, it gets increasingly more difficult when the noise level rises, as you would expect. But the expected measurable rate drops pretty fast, as we found out. We calculated this using the distance vs. noise relationship that we obtained for this setup. The results are shown in table 2:

Table 2

Noise level (mV):	Rate (events/day):
3	0.4000
4	0.2500
5	0.1700
7	0.1000
10	0.0500
20	0.0160
30	0.0078
40	0.0047
50	0.0031

So in Argentina, where the noise level is around 3 mV, we expect to detect about 2 showers every 5 days, which is reasonable to work with. But here in Nijmegen, with at least 30 mV worth of noise, the expected rate is only 1 shower in 128 days, at the most. It goes without saying that this is not a very practical rate.
But on the other hand, it is not impossible either to detect showers here through radio detection. We have shown a few examples of signals that could very well be from cosmic rays, even though we can not be sure yet, because for that we would have to use more than one antenna.
Therefore we have to conclude that, while it is theoretically possible to use radio detection of cosmic rays in the Netherlands, you have to be very patient. It is definitely not a suitable alternative to remote areas like Argentina.